Article citation info:
Kaźmierski B, Kapusta ŁJ. Numerical evaluation of urea-mixing devices for close-coupled selective catalytic reduction systems. Combustion Engines. 2023;193(2):84-93. https://doi.org/10.19206/CE-162624

Bartosz KAŹMIERSKI
Łukasz Jan KAPUSTA

Combustion Engines
Polish Scientific Society of Combustion Engines

Numerical evaluation of urea-mixing devices for close-coupled selective catalytic reduction systems

ARTICLE INFO

Received: 14 January 2023
Revised: 13 March 2023
Accepted: 26 March 2023
Available online: 7 April 2023

The following research presents a numerical evaluation of existing and conceptual urea-mixing devices used in close-coupled (to the engine) selective catalytic reduction (SCR) systems. The analysis was aimed at the assessment of urea-mixing devices that could considerably enhance the reduction of nitrogen oxides from the diesel-engine combustion process under a wide range of operating conditions, including cold starts. The analysis showed that replacing blade-equipped static mixers with perforated stationary mixing devices may provide a more uniform spatial distribution of ammonia at the inlet to the SCR catalyst and reduce pressure drops generated by mixing devices. Moreover, the conceptual mixing devices, based on combinations of the blade and perforated mixers to develop intensive turbulence, enabled the increase of the mixing length leading to effective decomposition of the urea-water solution (UWS), and provided uniform spatial distribution of ammonia, even for the small-sized mixing systems. However, the intensive mixing was often associated with a significant rise in the pressure drop.

Key words: *urea-water solution, urea mixer, selective catalytic reduction, SCR*

1. Introduction

The continuing use of diesel engines has become questionable due to the emission of harmful substances such as nitrogen oxides (NO_x). However, current exhaust gas aftertreatment systems enable a significant NO_x reduction, providing that they work under proper conditions, including the appropriate system temperature. One of the most effective NO_x abatement methods is selective catalytic reduction [25]. However, SCR systems are efficient only if the temperature of the substrate lies within a specific range [4, 34], which is dependent on the catalytic coating. Additionally, the temperature of the flue gas needs to be high enough to provide water evaporation and thermal decomposition of urea.

In a typical automotive SCR system, UWS is supplied upstream to the SCR catalyst using low-pressure injectors and immediately mixes with the relatively hot exhaust gas. Each single UWS droplet undergoes a process in which the water evaporates first [38, 48]. When a particle mostly composed of urea reaches a sufficiently high temperature (higher than 152°C [45]), chemical reactions occur. The primary reaction is thermolysis, expressed by Eq. (1):

$$(NH_2)_2CO \rightarrow NH_3 + HNCO \quad (1)$$

The generated ammonia (NH_3) and isocyanic acid (HNCO) are mixed with the exhaust gas, and the mixture enters the SCR catalytic converter, where the HNCO is converted into ammonia in a hydrolysis reaction (Eq. (2)):

$$HNCO + H_2O \rightarrow NH_3 + CO_2 \quad (2)$$

The ammonia developed in the thermolysis and hydrolysis is used to reduce the ammonia oxides to water and nitrogen, according to the governing chemical reactions (Eq. (3–5)):

$$4NO + 4NH_3 + O_2 \rightarrow 4N_2 + 6H_2O \quad (3)$$

$$2NO_2 + 4NH_3 + O_2 \rightarrow 3N_2 + 6H_2O \quad (4)$$

$$NO + NO_2 + 2NH_3 \rightarrow 2N_2 + 3H_2O \quad (5)$$

In order to reduce heat losses, the current SCR systems are combined into close-coupled modules containing diesel oxidation catalysts (DOC), diesel particulate filters (DPF), SCR converters and ammonia clean-up catalysts (CUC). Moreover, DPF and SCR catalysts are commonly integrated into one catalyst, referred to as an SDPF (SCR-coated diesel particulate filter). This SCR system's size reduction and location close to the engine both enable a decrease in the time required to achieve a suitable temperature inside a catalytic converter [31]. Moreover, an increased operating temperature before the SDPF catalyst favours UWS decomposition [4]. However, the system's size reduction shortens the droplets' pathlines, adversely affecting UWS decomposition before reaching the SCR catalyst.

The concept of the SCR system implies that accurate dosing of the UWS to properly match the amount of NO_x could lead to the complete conversion of nitrogen oxides into non-toxic substances. Therefore, assuming the perfectly uniform distribution of the velocity of the exhaust gas entering the SCR catalyst, it is also important to reach a uniform distribution of ammonia, achieved by the mixing process of UWS droplets and their by-products with the flue gas. However, the uniformity of gas velocity or ammonia distribution is often far from ideal, particularly regarding the wide span of operating conditions of diesel engines used in vehicles and transportation machines. Moreover, the efficiency of the conversion of UWS to ammonia (reactions (1)–(2)) is imperfect. Finally, the reactions (3)–(5) are not the only reactions occurring in the SCR systems as biuret, ammelide and other by-products are produced under certain conditions [17, 54], and they may occur as solid deposits

[54]. Payri et al. [42] also pointed out the importance of the UWS injector's position and its direction in aftertreatment system-relevant conditions, which affect the ammonia generation. The importance of the injector's direction is in accordance with our previous numerical study [21], which showed that it needs to be altered when the spray properties (most importantly, droplet size distribution) are changed. This was caused by the momentum exchange between droplets and cross-flowing gas, leading to the spray drift [13].

An effective way to enable more complete UWS decomposition is the application of static mixers [14], which also enhance spatial mixing of UWS droplets and their by-products with exhaust gas. The most common forms of static mixers are blade-based and baffle mixers aimed at vortex generation [50]. The advantage of blade mixers is their simplicity and the possibility of the use of the blades as impingement plates for droplets [47]. This may lead to droplet break-ups and the reduction of their size [28]. Additionally, static mixers reduce the velocity deviations of the gas entering the SCR catalyst [39]. On the other hand, blade-equipped mixers tend to work properly only under specific operating conditions [49], including with a suitable gas mass flow rate and temperature. While the first aspect influences the mixing (too strong or weak vortices may increase the local concentration of ammonia at the SCR's inlet), the temperature governs the UWS decomposition and evaporation of potentially occurring liquid film. Moreover, the blade-equipped mixers may not be easily adaptable to different spray characteristics, such as those attained through flash boiling [21].

Tan et al. [47] stressed the positive influence of the turbulence intensity increased by mixers on the UWS decomposition. Capetillo et al. [7] carried out numerical research to assess the impact of the blade angle, blade number and mixer's location in an SCR system equipped with a static mixer. In the case of the considered conditions, the biggest influence on the ammonia uniformity, pressure drop and liquid film's formation was observed to come from the angle of the blades. Shortening the distance between the injector and mixer also had a positive effect on NH_3 uniformity; however, this factor was of low importance. This shorter distance additionally enabled a slight reduction in the pressure drop. Ye et al. [50] analysed the influence of the mixer type, the number of mixers and the injector's position in the SCR system. Two types of mixers were considered – a conventional blade mixer and a conventional baffle mixer. The application of a single baffle mixer downstream to the injection or any two mixers enabled the increase of the ammonia uniformity index even by 136.4%, as well as an increase in ammonia generation. Nevertheless, the double-mixer configurations resulted in a considerable rise in overpressure. Mehdi et al. [33] performed a numerical study on blade and baffle mixers' performance in a marine SCR system. A combination of two mixers ensured the best uniformity of velocity and ammonia concentration. Even though the UWS residence time was the shortest for this configuration, the urea conversion was the most efficient. Two types of mixers were numerically tested by Park et al. [40], namely, a regular baffle-shaped mixer and a version generating swirl. The latter provided the best compromise between the ammonia uniformity index and the pressure drop.

Hui et al. [18] pointed out that it is difficult to achieve the uniform distribution of NH_3 using hole-type UWS injectors. While, Jang et al. [19] observed a decrease in exhaust gas temperature in a marine SCR system equipped with a mixer, along with a rise in the ammonia concentration. This was attributed to the endothermic thermolysis reaction and the increased area where the reaction took place. The application of a mixer particularly enhanced the uniformity of the NH_3 distribution, while its impact on the uniformity of the velocity distribution and ammonia concentration was much lower.

Another solution proposed for SCR mixers is a perforated tube inside which the UWS injection takes place, with only a part of the exhaust gas entering the tube. Therefore, the momentum exchange between the UWS droplets and gas is reduced, which in turn reduces the impact of the gas mass flow rate on the trajectories of the droplets. The main advantage of perforated mixers is their versatility. It is assumed that the adequately designed perforated mixer may enable more efficient UWS decomposition under a wider range of operating conditions than a blade mixer. The main drawback, in turn, is an increased tendency to liquid film deposition within the perforations, as well as raised manufacturing complexity. Zhang et al. [51] numerically analysed baffle-type and blade-based mixers, using a perforated tube as a secondary mixer at the inlet to the diffuser. The combination of the main, baffle-type mixer with additional blades at the circumferential part and the secondary perforated-tube-mixer provided the most uniform ammonia distribution, the lowest pressure drop and the lowest mass of the solid deposit under the tested conditions. Different mixers were also numerically tested and compared in an SCR system employing blade or baffle mixers with an additional perforated tube by Fu et al. [11]. The simple double-bladed design generated much higher backpressure and film deposition than other designs. The baffle mixer led to the lowest uniformity index of ammonia at the SCR's inlet, which was attributed to the least intense turbulence. However, this design generated the lowest pressure drop and provided the highest NO_x conversion efficiency due to the lowest film generation and the most complete droplet evaporation. Zhao et al. [52] presented an SCR mixer that generates spiral flow, elongating the droplets' pathlines, despite the small overall volume of the mixer. The mixer was enclosed by the perforated diffuser with a baffle-type mixer in the central part, which was aimed at uniform dispersing of the ammonia and balancing the centrifugal effect caused by the spiral part. In their numerical analysis, Kaźmierski et al. [24] utilised the concept of the perforated mixer equipped with guiding vanes outside the tube to develop the washing flow of the exhaust gas. This mixing device was used in a close-coupled SCR system providing a relatively high NH_3 uniformity index and low liquid film formation. The complex perforated mixer equipped with the vanes and the spinning disk was used by Huang et al. [16] in their numerical analysis of an SCR system, in which they determined the uniformity index of the ammonia, the pressure drop and the solid deposit formation, including the

species' analysis. The authors stated that additional holes in the ring baffle enabled the reduction of the system's overpressure. Interestingly, the number of vanes had a low impact on the pressure drop. Moreover, it was found that the number of swirling vanes could improve the ammonia uniformity at the SCR's inlet; however, exceeding a certain number would deteriorate it [16]. Therefore, the careful design process of mixers is crucial for beneficial selective catalytic reduction. The liquid film and solid deposit formation process was numerically investigated by Li et al. [30] for the perforated mixer. The authors observed that in the case of relatively high temperatures the mixer's geometry had a primary influence on the deposit's location; while at lower temperatures, its location was more dependent on the position and orientation of the UWS injector.

This efficient mixing performance with low deposit formations has also been attained with unconventional mixers by other researchers. Millo et al. [37] presented two unconventional SCR mixers generating separated vertices at gas and spray zones that provided an NH_3 uniformity index of 96–98%, and a time-averaged NO_x conversion efficiency of 98–99%, for the gas mass flow rate of 125 kg/h and temperature of 250°C. Michelin et al. [35] developed and tested an innovative design of an SCR mixing device, characterised by its minimised volume to enable maximum compactness of close-coupled systems. The operating principle was the development of a spiral gas trajectory and subsequent increase in the evaporation length for the UWS droplets. The evolution of innovative SCR mixers was also presented by Michelin et al. [36], comprising asymmetric vortex generation from a U-shaped design with swirling vanes or symmetric-vortex generation via an internal catcher and baffles. Moreover, the underfloor SCR layouts, including additional heating, were compared with close-coupled systems. The modern close-coupled layout provided the highest NO_x conversion efficiency for the same mixing device [36]. Another example of an unconventional solution was a mixer-less SCR system dedicated to close-coupled layouts [23]. Efficient mixing was attained at diverse mass flow rates of the flue gas and different spray set-ups (conventional and flash-boiling injections). The mixing performance was assessed by the uniformity index of the ammonia distribution; it was attributed to the intensive turbulence reached in the mixing chamber, and due to the abrupt change of the flow direction. Zheng et al. [53] developed conical-blade, two-stage and butterfly mixers for SCR applications. The butterfly-shaped mixer provided particularly high ammonia uniformity and NO_x reduction, as well as relatively low pressure drops at the same time. The authors stressed that SCR mixers are incapable of reaching a high performance in all applications and conditions. Kulkarni et al. [28] proposed reducing UWS surface tension by adding surfactant. The authors stated that this addition might improve mixing in urea-SCR systems due to the enhanced evaporation, attributed to the increased spreading factors of the droplets (ratios of a lamella size to the droplet diameter before the collision) and the narrower droplet size distributions reached for the secondary droplets.

The aforementioned investigations indicate there is no single, unquestionably best solution for a urea-SCR mixer intended for close-coupled applications. Therefore, the aim of this research was to find the answer to the following problem: what form of a urea-SCR mixer is the most efficient in terms of mixing performance and pressure drop? For this reason, seven different mixing devices were numerically tested in the same simplified close-coupled SCR system. All the mixing devices were supposed to be universal solutions; hence, specific, unconventional designs adjusted to any particular applications were not considered. The conclusions, including the greatest overall performance of the perforated mixers, are expected to orient the future design process of SCR mixers and increase the effectiveness of selective catalytic reduction systems.

2. Methods

The following research comprises a numerical analysis of the distinct forms of static mixers placed in the same close-coupled SCR system. The system was simplified to exclude the influence of complex geometrical shapes on the results. The presented analysis was performed numerically based on the Reynolds-averaged Navier-Stokes (RANS) approach with the k-ζ-f turbulence model [15], and the hybrid (compound) wall treatment [15, 43] applied.

2.1. Simulated system

The considered SCR system design was based on the close-coupled systems which have recently been widely used in the automotive industry, due to their provision of reduced heat losses [31], faster heating of the system and improved NO_x conversion efficiency [36]. The first component of the computational domain was the stabilisation volume followed by the diesel oxidation catalyst (DOC). Downstream from the DOC, there was an investigated mixing device, inside which UWS was injected. The external shape of the system was unchanged. The only difference between the investigated solution was the design and arrangement of the internal mixing elements. In the base model M0 (Fig. 1a), a simple elbow connected the DOC and SDPF catalysts with no additional mixing device placed inside. In the M1 model (Fig. 1b), the mixing element was a simple blade-based mixer, with a 45° inclination angle of each blade. In the M2 model (Fig. 1c), a combination of two analogous mixers was used, with the second mixer being counter-rotating. Such a layout aimed to increase the turbulence intensity by reversing the direction of the vortex generated by the first mixer. In the M3 model (Fig. 1d), the perforated tube was applied. The tube was equipped with holes around the bottom part. The upper part contained two symmetrical slots, which were shifted towards the inlet to work as a gas intake for the mixer's tube. Therefore, it was intended that only a minor fraction of the exhaust gas would enter the mixing tube so that diverse operating mass flow rates of gas would not cause a spray drifting effect. The UWS droplets were thereby formed in the high-temperature zone, without a too excessive momentum exchange between gas and droplets, favouring reduction of the liquid film and UWS decomposition. Then, the mixture of the flue gas and urea or decomposed by-products escaped the tube via the holes, forcing changes in flow

direction and increasing the ammonia spatial uniformity. The analogous mixer was employed in the M4 model (Fig. 1e), however the perforations were made exclusively in its lower part located farther from the inlet and outlet. Hence, the escaping mixture of the flue gas and urea/ammonia was forced to change its flow direction completely, and the pathlines became elongated and more uniformly spread. The mixers M5 (Fig. 1f) and M6 (Fig. 1g) were the hybrid mixing devices that posed combinations of M1 with M3, and M1 with M4, respectively. They were aimed at the generation of the swirling flow exclusively outside the tube.

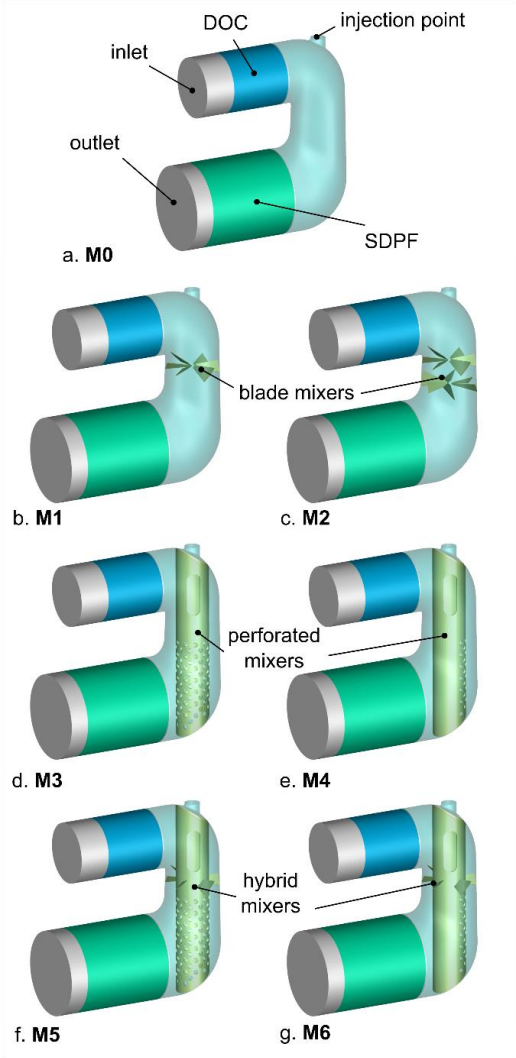

Fig. 1. The geometrical models of close-coupled SCR systems used in the simulation: a. system without mixing elements; b. single-bladed mixer; c. double, counter-rotating blade mixers; d. perforated mixer; e. partially perforated mixer; f. hybrid, blade-perforated mixer; g. blade-partially-perforated mixer

2.2. Computational mesh

A numerical mesh was generated in the AVL FAME™ M 2021 meshing module. The mesh consisted of polyhedral cells to reduce their sensitivity to numerical diffusion and reproduce sharp edges, while simultaneously maintaining their adequate quality. The boundary layer consisted of six layers with a total thickness of approximately 3 mm with automatic adjustments. The base cell size of the polyhedral cells was 5 mm, reduced to 3 mm in proximity of the walls. The mixers' surfaces were refined to reach the cell size of approximately 2 mm to properly simulate the behaviour of impinging droplets and the possible liquid film. Additionally, the mesh was refined with 1-mm cells within the primary injection zone (see. Fig. 2):

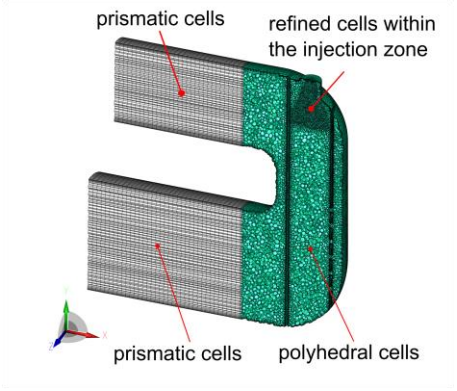

Fig. 2. The cross-section of the computational mesh of the SCR system

2.3. Numerical cases

The operating conditions were selected to reflect the conditions in exhaust systems of medium-sized passenger cars under high and medium loads [20]. The considered mass flow rate of exhaust gas was 300 kg/h (OP1) and 150 kg/h (OP2). In the case of both operating points (OPs), the gas temperature was the same: 400°C. The relatively high temperature favoured the evaporation of water from UWS droplets and accelerated urea decomposition, therefore, minimising the risk of liquid film occurrence. For this reason, the comparison of various types of SCR mixers was focused exclusively on the mixing performance and not on the tendency to generate liquid or solid deposits. Since the spray was modelled according to the Eulerian-Lagrangian approach (see section 2.4), spray properties were used as input data, and they were derived from previous experimental measurements of the two-hole injector (Bosch 0444025030) [21, 22], working under the injection pressure of 5 bar. The constant injection frequency of 4 Hz was assumed in accordance with the previous injector's mass flow measurements [21]. The amount of the urea-water solution per single injection was dependent on the injector's opening time. The UWS mass per injection was calculated based on the assumed NO_x concentration (specifically: nitric oxide concentration) of 150 ppm, corresponding to the medium load of a mid-sized passenger car (with exhaust gas recirculation) in urban traffic conditions [9]. The replacement of NO_x only with nitric oxide was based on the experimental measurements [32] that indicated the prevailing composition of NO over NO_2 at the catalyst's inlet. Nonetheless, the NO_x conversion was not simulated; hence, the exact NO_x composition had a negligible effect on the results. The summary of the operating conditions, including the UWS dosing, is presented in Table 1.

Table 1. The summary of operating conditions

Operating point	Gas mass flow rate	Gas temperature	Injector's opening time	UWS mass per injection
OP1	300 kg/h	400°C	22.77 ms	9.99 mg
OP2	150 kg/h	400°C	11.39 ms	5.00 mg

The dimensions of the catalytic converters, namely the DOC and SDPF, were defined based on similar catalytic converters used in mid-sized passenger cars. They were modelled as porous zones with a predefined, longitudinal flow direction. The pressure drops in the substrates were determined by Forchheimer's formula [10], which in the case of unidirectional flow, is expressed by Eq. (6).

$$\frac{dP}{dx} = -\alpha \cdot \mu \cdot u - \zeta \cdot \frac{\rho}{2} \cdot u^2 \tag{6}$$

where: x – distance along the flow direction; α – viscous loss coefficient; μ – dynamic viscosity; u – local gas velocity (unidirectional) inside the porous object; ζ – inertial loss coefficient; ρ – gas density. In the case of the following analysis, the α and ζ coefficients were also adopted based on similar catalytic converters from mid-sized passenger cars, with an adaptation to the specific porosity fraction.

The porosity fraction (ratio of the open volume to the whole volume of a substrate) was assumed as unity to simplify the simulated system to the maximum extent and focus exclusively on the differences caused by the various mixers. The properties of the substrates (in this case: porous objects) are presented in Table 2.

Table 2. Properties of the substrates

Catalytic converter	Length	Diameter	Viscous loss coefficient	Inertial loss coefficient	Porosity fraction
DOC	150 mm	100 mm	$2 \cdot 10^7 \frac{1}{m^2}$	$40 \frac{1}{m}$	1
SDPF	180 mm	140 mm	$10^8 \frac{1}{m^2}$	$500 \frac{1}{m}$	1

Multiple parameters can be used to evaluate the performance of SCR systems. These are: the efficiency of NO_x conversion; the uniformity of the ammonia (reducing agent) and gas velocity entering the SCR catalyst; the total pressure drop; the liquid film formation; and the risk of deposit formation.

While the NO_x conversion efficiency reflects the overall effectiveness of the system, it also depends on the NH_3 uniformity and liquid film deposition. Hence, the uniformity of the reducing agent is a direct and independent parameter, and it was indicated as the most important criterion by Zheng et al. [53]. Moreover, Xu et al. [49] showed that the ammonia uniformity at the SCR's inlet is linked with NO_x conversion efficiency. In the present analysis, the comparison of different mixer designs in close-coupled SCR systems was made based on the uniformity index of the ammonia concentration in the inlet to the SCR catalyst (approximately 10 mm behind the front surface of the porous zone – see Fig. 3). The uniformity index of the velocity was also determined in the same control section according to Eq. (7):

$$\gamma = 1 - \frac{\sum(|u_i - \bar{u}| \cdot A_i)}{2 \cdot \bar{u} \cdot A} \tag{7}$$

where: u_i – local velocity component in the i-th cell; $\bar{u}$ – area-averaged velocity within the whole control surface; A_i – area of the i-th cell; $A = \sum A_i$ – total area of the control surface.

It is to be noted that the calculation of the NH_3 uniformity index was based on Eq. (7); however, it was averaged in time and space. Moreover, the pressure drop of the mixing device was evaluated (defined here as the difference between the total pressure at the outlet at the DOC and inlet to the SDPF catalyst). Since negligible liquid film formation was expected, and the velocity uniformity index was close to 100%, the NO_x conversion would depend mostly on the spatial distribution of NH_3 within the SDPF's inlet and the urea-to-ammonia conversion. Therefore, the NH_3 uniformity index was assumed as the most accurate indicator of the mixer's effectiveness. Additionally, considering the hydrolysis reaction, Eq. (2) or NO_x reduction was unnecessary. Hence, the assumed concentration of NO_x was used exclusively to determine the dosing of UWS.

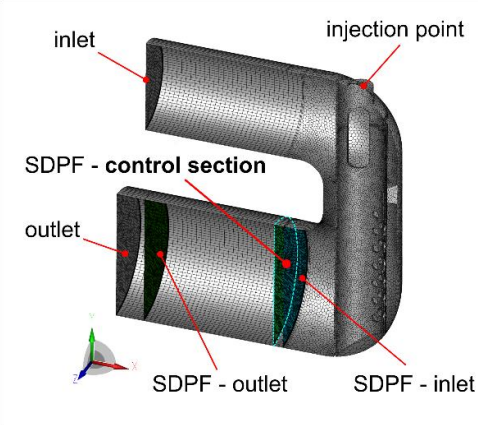

Fig. 3. The cross-section of the SCR system with the visible control section located 10 mm downstream from the SDPF's inlet

2.4. Computational mesh

The injection of the urea-water solution was simulated employing a discrete droplet model (DDM) [8], which is the Eulerian-Lagrangian particle tracking method. Droplets were randomly dispersed in the space starting from the predefined nozzles' locations. To reduce the numerical effort, droplets of similar properties are grouped into parcels in the DDM approach, and such parcels are tracked instead of single droplets. In a typical DDM approach in low-pressure UWS sprays, it is assumed that the size of the introduced droplets is the size reached after the primary break-up. The secondary break-up is not present due to low Weber numbers [1], and the application of the break-up models for such low Weber numbers can be unsuccessful [41].

Therefore, droplet size measurements are required to model the droplet size distribution properly. The most suitable measuring methods are optical laser techniques, including phase Doppler anemometry, high-resolution laser backlight imaging and high-speed microscopic imaging [6]. In this study, a pre-calibrated spray model was taken from previous work [21]. The calibration was done for the commercial two-hole UWS injector (Bosch 0444025030) experimentally tested in [21,22] using optical methods. The spray parameters used in the study here are shown in Table 3.

In order to increase the accuracy of the spatial droplet dispersion, two separated conical zones with individual droplet size distributions were defined for each spray plume, as initially proposed in [44]. These individual droplet size distributions (for each spray zone) were also derived from the research [21, 22] (Fig. 4).

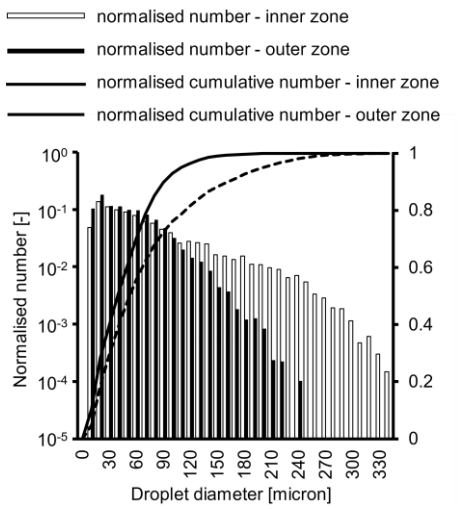

Fig. 4. The droplet size distributions of the two-zone representation of the spray used in simulations [21, 22]

The dynamics of the droplet was evaluated employing the Schiller-Naumann drag-estimation approach [46] and the Kuhnke splashing model [27] extended by Birkhold [2] to ultimately account for the droplet deposition, splashing, rebound, and break-up, but also partial rebound and partial break-up. Both spray and liquid film decomposition were modelled by the approach proposed by Birkhold [3] with the reaction's (thermolysis) activation energy and frequency factor fitted to Kim's experiment [26]. Moreover, the turbulent dispersion model was taken into account in terms of the droplets' behaviour [12].

Table 3. The summary of spray properties

Spray property	Value
Initial velocity	31.1 m/s
Inner cone angle	2°
Outer cone angle	5°
UWS mass ratio (outer-to-inner conical zones)	0.266

3. Results

A comparative analysis of the universal mixing devices dedicated to close-coupled SCR systems was performed. The effectiveness of a particular mixer was assessed based on the uniformity index of the ammonia 10 mm after the SDPF's (SCR's) inlet, and on the pressure drop of the mixing device. Additionally, the values of the velocity uniformity index measured 10 mm behind the SDPF's inlet were compared. The results showed that no liquid film was observed in any of the considered cases, which was expected due to the relatively high temperature of the exhaust gas.

3.1. The ammonia uniformity

The time-averaged concentration of the ammonia at the SDPF's control section (Fig. 3), obtained after four UWS injections, is presented in Fig. 5 (operating point 1) and Fig. 6 (operating point 2). The number of simulated injections was selected as a compromise between the computational time and the stabilisation of the investigated parameters. Lee [29] addressed the different behaviour of the droplets after the first injection compared to after the following injections. Droplets from the first injection flowed backwards and mixed with the droplets from the second injection. Later, the droplets from the following injections were mixed, and many of them were registered at the inlet of the mixer. However, the increased residence time was reported as advantageous for water evaporation and urea thermolysis [29].

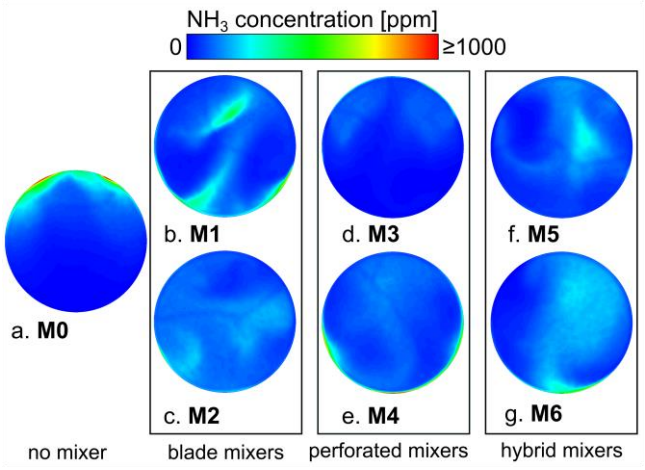

Fig. 5. Ammonia distribution at the control section located 10 mm downstream from the SDPF's inlet; OP1

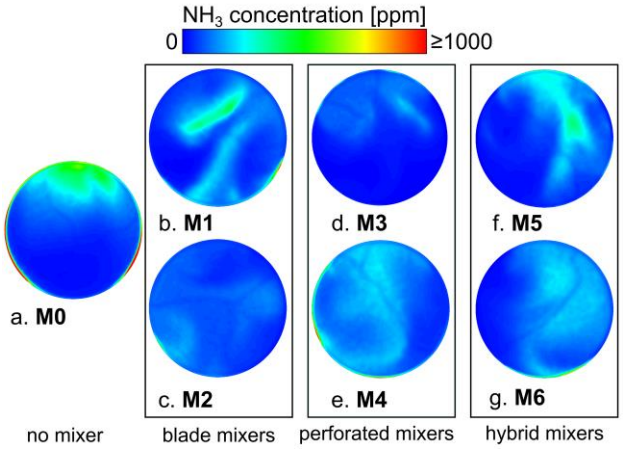

Fig. 6. Ammonia distribution at the control section located 10 mm downstream from the SDPF's inlet; OP2

It is seen that there were highly concentrated ammonia spots at the circumference of the SCR system without any mixing element; and those locations were completely different in the cases of the high (Fig. 5a) and low (Fig. 6a) mass flow rates of flue gas. This suggests that the distribution of ammonia resulted from the intensive momentum exchange between droplets and gas; since the velocity distribution maps (Fig. 7) did not indicate significant differences between operating points 1 and 2. Moreover, the higher velocity values in Fig. 7 did not correspond with the high-ammonia-concentration spots (Fig. 5a and Fig. 6a).

The application of the blade mixer (Fig. 5b and Fig. 6b) significantly improved the spatial distribution of ammonia. However, the diagonal traces of the increased NH_3 concentration were visible as a result of the generated swirl (Fig. 5b and Fig. 6b). The double-bladed mixer (M2) and the fully perforated mixer (M3) left the least distinguishable

traces of high-ammonia concentration, except for the circumference of the control section (Fig. 5c, d and Fig. 6c, d). The partially perforated mixer (M4) and hybrid mixers (M5, M6) caused the occurrence of undulated ammonia traces (Fig. 5e–g and Fig 6e–g), which were the effect of the sudden deflection of UWS/ammonia pathlines due to perforations (M4) or due to the single blade mixer (M5, M6).

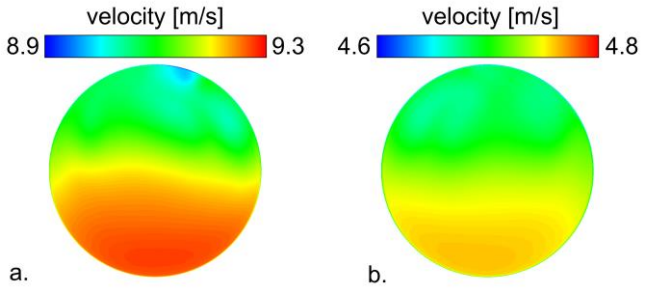

Fig. 7. Velocity distribution at the control section located 10 mm downstream from the SDPF's inlet; M0; a. OP1, b. OP2

The registered ammonia uniformity index reached similar values for both operating points 1 and 2 (Fig. 8). Additionally, the common relationships between those values for different mixing devices remained similar in the case of OP1 and OP2 (Fig. 8). The SCR system without any mixing elements (M0) resulted in an ammonia uniformity index of approximately 50%, which is an unacceptably low result. The application of the conventional, blade-equipped mixer (M1) raised the γ_{NH3} index to 72–74%. In the case of the double-bladed mixer (M2), with the second mixer generating a swirling flow in the opposite direction, γ_{NH3} was considerably increased to approximately 86% for both OP1 and OP2, which is an acceptable value in industrial applications [5]. However, it is to be noted that the presented SCR systems were simplified to the maximum extent to compare exclusively the mixer's performance, which explains the relatively low overall scoring. The application of the perforated mixer, with the holes around the whole of the lower part of the tube's surface, did not improve the γ_{NH3} much (64%). Nonetheless, in the case of perforations made exclusively at a further distance from the SDPF (M4), which hindered the direct outflow from the tube's interior to the catalyst and elongated the pathlines of the flue gas-UWS mixture, it led to a rise in the NH_3 uniformity index to 74–79%.

Finally, the blade mixer used in model M1 was combined with perforated mixers (M3 and M4, respectively). The first combination (M5) resulted in γ_{NH3} of the same level as for the partially-perforated mixer (M4) – approximately 75–77%. A slightly positive influence from the combination of the blade mixer with the fully perforated tube was observed. However, the improvement was minor compared to the blade mixer alone ($\gamma_{NH3} \approx 73\%$ for blade mixer vs. $\gamma_{NH3} \approx 76\%$ for the first hybrid mixer).

Almost the same value of γ_{NH3} as in the case of the M5 was reached by the last mixer (M6). The combination of the partially perforated tube with the blade mixer was ineffective as it significantly increased the manufacturing complexity, while it did not bring an improvement compared to the partially perforated mixer alone. This is in accordance with the analysis by Xu et al. [49], who tested not only single, unconventional urea mixing devices, but also their combinations. They reported that the single, counter-swirl mixer produced a superior performance compared to other unconventional mixers and provided the highest NO_x conversion efficiency, the lowest ammonia non-uniformity index, and a relatively low pressure drop.

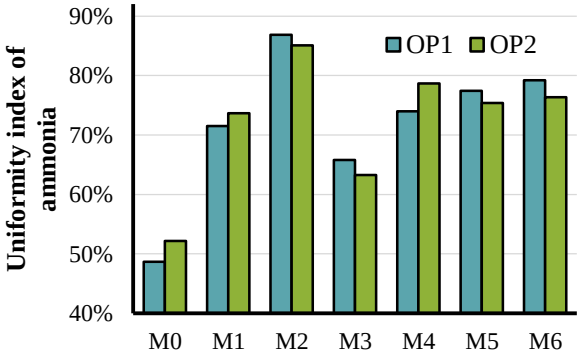

Fig. 8. Ammonia uniformity index at the control section located 10 mm downstream from the SDPF's inlet

3.2. Pressure drop

The second-ranked criterion in the following research was the pressure drop generated by the mixing devices, which was calculated as the difference between the total pressure at the outlet of the DOC and at the inlet to the SDPF catalyst. The results are presented in Fig. 9. According to the expectations, the common relationships between the pressure drops generated by the individual mixers are analogous for both operating points 1 and 2. It is seen that the pressure drop generated by the single blade mixer (M1), fully perforated mixer (M3) and partially perforated mixer (M4) are almost the same: ~200 Pa at operating point 1 and ~60 Pa at operating point 2. The negligible influence of the number of perforations on the pressure drop resulted from the fact that only a certain amount of the flue gas entered the perforated tube, while the majority washed over it from the outside. The increase of the number of blade mixers to two, with the forced change in the swirl's direction by the second mixer (M2) led to a tremendous increase in the pressure drop – more than twofold compared to the version with a single blade mixer (M1). The combination of the single blade mixer with perforated mixers (M5 and M6) also led to a significant rise in the pressure drop (from ~200 Pa for M1 at operating point 1 to ~360 Pa and ~430 Pa for M5 and M6, respectively). However, it is to be noted that the ammonia uniformity index was not improved noticeably by the hybrid mixing devices, which makes this type of design questionable. Moreover, in the case of the hybrid mixers, the number of perforations resulted in a difference in the pressure drop, being higher for the reduced number of perforations (M6). This might have come from the synergy between the swirling flow outside the tube and the outflow from the tube's holes. Additionally, the increased sensitivity of this type of hybrid design (M5, M6) to the working conditions could occur during real driving cycles.

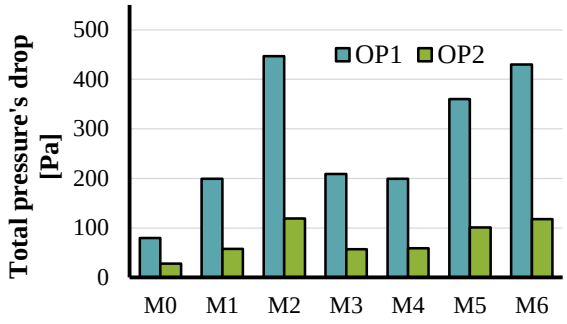

Fig. 9. Pressure drop generated by each UWS mixing device

3.3. Uniformity of velocity

Even though the analysed SCR systems were simplified to the maximum extent, the velocity uniformity index determined 10 mm after the SDPF's inlet exceeded 99% in all the considered cases (Fig. 10). Similarly to the ammonia uniformity index, the relationship between the values reached by specific mixers is analogous at operating points 1 and 2. Surprisingly, the uniformity index registered for the M0 geometry is the second highest, which may result from the lack of geometrical contractions and highly uniform velocity field within the system's inlet and DOC catalyst. However, the achievement of the highly uniform velocity and temperature fields at the catalyst surface requires a lower effort compared to the uniformity of the reducing agent, as reported by Zheng et al. [53]. Nonetheless, all the values of the velocity uniformity index are close to unity, and the exact comparison requires caution, since the differences might be a result of numerical solutions.

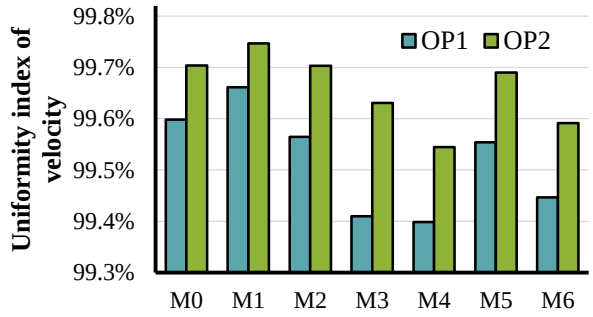

Fig. 10. Velocity uniformity index at the control section located 10 mm downstream from the SDPF's inlet

4. Conclusions

This research was aimed at an evaluation of urea-mixing devices that could considerably enhance the reduction of nitrogen oxides in close-coupled SCR systems. Seven different mixing devices were numerically tested in the same aftertreatment system and under the same operating conditions corresponding to high- and medium-load engine operation. The analysis led us to the following conclusions:

- Each mixing device improved the ammonia uniformity index.
- All mixing devices provided a velocity uniformity index exceeding 99%.
- All systems were almost insensitive to changes in the operating conditions (exhaust gas mass flow rates).
- The SCR system without mixing elements (M0) provided a highly uniform velocity field; however, the uniformity index of ammonia measured in the same control section was only 50%.
- The biggest improvement in the ammonia uniformity index was observed for the double counter-rotating mixer ($\gamma_{NH3} \approx 86\%$). However, this design (M2) generated the highest pressure drop (more than twofold compared to the version with the single blade mixer).
- The partially perforated mixer (M4) enabled the achievement of a high ammonia uniformity index (74–79%), while generating a relatively low pressure drop; which was the same as for the single blade mixer (M1).
- The hybrid mixers provided a relatively high but not improved ammonia uniformity index compared to the single blade or perforated mixers, but they did cause a significant rise in the pressure drop.
- Perforated mixers alone are expected to be used as one of the leading solutions in future SCR systems, providing a compromise between great mixing performance and manufacturing complexity.

Acknowledgements

The work was supported by the National Centre for Research and Development (NCBiR), grant no. MAZOWSZE/0101/19-00, programme "Ścieżka dla Mazowsza", project budget: 9 880 490.25 PLN.

Numerical analysis was conducted under the AVL University Partnership Program.

Nomenclature

A	total area of the control surface
A_i	area of the i-th cell
CUC	clean-up catalyst
DOC	diesel oxidation catalyst
DPF	diesel particulate filter
HNCO	isocyanic acid
NO_x	nitrogen oxides
SCR	selective catalytic reduction
SDPF	SCR-coated diesel particulate filter
u	local gas velocity (unidirectional) inside the porous object
$\bar{u}$	area-averaged velocity within the whole control surface
u_i	local velocity component in the i-th cell
UWS	urea-water solution
x	distance along the flow direction
α	viscous loss coefficient
ζ	inertial loss coefficient
μ	dynamic viscosity
ρ	gas density

Bibliography

[1] Bai C, Liu K, Zhao T et al. Study on spray characteristics and breakup mechanism of an SCR injector. Appl Sci. 2022;12(18). https://doi.org/10.3390/app12189387

[2] Birkhold F. Selektive katalytische Reduktion von Stickoxiden in Kraftfahrzeugen: Untersuchung der Einspritzung von Harnstoffwasserlösung. Dissertation. Shaker Verlag GmbH, 2007.

[3] Birkhold F, Meingast U, Wassermann P et al. Modeling and simulation of the injection of urea-water-solution for automotive SCR DeNOx-systems. Appl Catal B: Environmental. 2007;70(1-4):119-127. https://doi.org/10.1016/j.apcatb.2005.12.035

[4] Börnhorst M, Deutschmann O. Advances and challenges of ammonia delivery by urea-water sprays in SCR systems. Prog Energ Combust. 2021;87:100949. https://doi.org/10.1016/j.pecs.2021.100949

[5] Boruc Ł, Rogoz R, Bachanek J et al. An experimental facility for rapid testing of SCR systems. SAE Technical Paper 2020-01-2192. 2020. https://doi.org/10.4271/2020-01-2192

[6] Bracho G, Postrioti L, Moreno A et al. Experimental study of the droplet characteristics of a SCR injector spray through optical techniques. Int J Multiphas Flow. 2021;135:103531. https://doi.org/10.1016/j.ijmultiphaseflow.2020.103531

[7] Capetillo AJ, Ibarra F, Stepniewski D et al. Multiphase modelling of SCR systems: using the Taguchi method for mixer optimisation. SAE Int J Engines. 2017;10(1):61-71. https://doi.org/10.4271/2017-26-0113

[8] Dukowicz JK. A particle-fluid numerical model for liquid sprays. J Comput Phys. 1980;35(2):229-253.

[9] Fernández E, Ortego A, Valero A et al. Suitability assessment of NO_x emissions measurements with PTI equipment. Vehicles. 2022;4(4):917-941. https://doi.org/10.3390/vehicles4040050

[10] Forchheimer P. Wasserbewegung durch boden. Zeitschrift des Vereins deutscher Ingenieure, 45th edition. 1901.

[11] Fu H, Huang Z, Tang C et al. Effect of mixer structure on liquid film formation and NO_x conversion efficiency in selective catalytic reduction system. Fuel. 2022;330:125405. https://doi.org/10.1016/j.fuel.2022.125405

[12] Gosman AD, Loannides E. Aspects of computer simulation of liquid-fueled combustors. J Energy. 1983;7(6):482-490. https://doi.org/10.2514/3.62687

[13] Górka K, Kaźmierski B, Kapusta ŁJ. Numerical analysis of the flow rig for UWS spray examination in exhaust system-relevant conditions. Combustion Engines. 2021;186(3):103-112. https://doi.org/10.19206/CE-141182

[14] Grout S, Blaisot J-B, Pajot K et al. Experimental investigation on the injection of an urea–water solution in hot air stream for the SCR application: evaporation and spray/wall interaction. Fuel. 2013;106(x):166-177. https://doi.org/10.1016/j.fuel.2012.09.022

[15] Hanjalić K, Popovac M, Hadžiabdić M. A robust near-wall elliptic-relaxation eddy-viscosity turbulence model for CFD. Int J Heat Fluid Fl. 2004;25(6):1047-1051. https://doi.org/10.1016/j.ijheatfluidflow.2004.07.005

[16] Huang H, Chen Y, Li Z et al. Analysis of deposit formation mechanism and structure optimization in urea-SCR system of diesel engine. Fuel. 2020;265:116941. https://doi.org/10.1016/j.fuel.2019.116941

[17] Huang H, Zhang L, Chen Y et al. Study on decomposition and by-products formation mechanism of urea solution impinging on heated plate in SCR system. Chemosphere. 2022;(309):136620. https://doi.org/10.1016/j.chemosphere.2022.136620

[18] Hui Z, Boyan X, Chuansheng W. Numerical simulation to reduce NO_x of diesel engine urea-SCR system. Open Mechanical Engineering Journal. 2014;8(2):643-647. https://doi.org/10.2174/1874155x01408010643

[19] Jang J, Na S, Roh H et al. Spraying and mixing characteristics of urea in a static mixer applied marine SCR system. Energies. 2021;14(18). https://doi.org/10.3390/en14185788

[20] Kandylas IP, Stamatelos AM. Engine exhaust system design based on heat transfer computation. Energ Convers Manage. 1999;40(10):1057-1072. https://doi.org/10.1016/S0196-8904(99)00008-4

[21] Kapusta ŁJ, Rogoz R, Bachanek J. Experimental and numerical study to evaluate the effect of flash boiling on urea-water solution sprays and SCR system performance. Atomization Spray. 2021;31(5):89-117. https://doi.org/10.1615/AtomizSpr.2021035461

[22] Kapusta ŁJ, Rogoz R, Bachanek J et al. Low-pressure injection of water and urea-water solution in flash-boiling conditions. SAE Int J Adv Curr Pract Mobility. 2020;3(1):365-377. https://doi.org/10.4271/2020-01-2110

[23] Kaźmierski B, Górka K, Kapusta ŁJ. A conceptual design and numerical analysis of the mixerless urea-SCR system. Combustion Engines. 2021;187(4):12-20. https://doi.org/10.19206/CE-140539

[24] Kaźmierski B, Kapusta ŁJ. The importance of individual spray properties in performance improvement of a urea-SCR system employing flash-boiling injection. Appl Energ. 2023;(329):120217. https://doi.org/10.1016/j.apenergy.2022.120217

[25] Kim HJ, Lee SH, Kwon SI et al. Investigation of the emission characteristics of light-duty diesel vehicles in Korea based on Euro-VI standards according to type of aftertreatment system. Energies. 2020;13(18). https://doi.org/10.3390/en13184936

[26] Kim JY, Ryu SH, Ha JS. Numerical prediction on the characteristics of spray-induced mixing and thermal decomposition of urea solution in SCR system. Proceedings of the ASME 2004 Internal Combustion Engine Division Fall Technical Conference. 2004:165-170. https://doi.org/10.1115/ICEF2004-0889

[27] Kuhnke D. Spray/Wall-Interaction Modelling by Dimensionless Data Analysis. Shaker Verlag GmbH, 2004.

[28] Kulkarni AP, Megaritis T, Ganippa LC. Impact dynamics and morphology of urea-water-solution droplets impinging on a hot plate under urea-SCR relevant conditions: influence of surface tension. Fuel. 2021;298:120671. https://doi.org/10.1016/j.fuel.2021.120671

[29] Lee C. Numerical and experimental investigation of evaporation and mixture uniformity of urea–water solution in selective catalytic reduction system. Transport Res D-Tr E. 2018;60:210-224. https://doi.org/10.1016/j.trd.2017.04.015

[30] Li M, Zhang Y, Liu X et al. Numerical investigation on the urea deposit formation process in a selective catalytic reduction system of a diesel engine based on a fluid–solid coupling method. ACS Omega. 2021;6(8):5921-5932. https://doi.org/10.1021/acsomega.1c00021

[31] Maizak D, Wilberforce T, Olabi AG. DeNOx removal techniques for automotive applications – a review. Environ Adv. 2020;2:100021. https://doi.org/10.1016/j.envadv.2020.100021

[32] Majewski WA, Ambs JL, Bickel K. Nitrogen oxides reactions in diesel oxidation catalyst. SAE Technical Paper 950374. 1995. https://doi.org/10.4271/950374

[33] Mehdi G, Zhou S, Zhu Y et al. Numerical investigation of SCR mixer design optimization for improved performance. Processes. 2019;7(3). https://doi.org/10.3390/pr7030168
[34] Mera Z, Fonseca N, López J-M et al. Analysis of the high instantaneous NO_x emissions from Euro 6 diesel passenger cars under real driving conditions. Appl Energ. 2019;242: 1074-1089. https://doi.org/10.1016/j.apenergy.2019.03.120
[35] Michelin J, Guilbaud F, Guil A et al. Advanced compact SCR mixer: BlueBox. SAE Technical Paper 2014-01-1531. 2014. https://doi.org/10.4271/2014-01-1531
[36] Michelin J, Nappez P, Guilbaud F et al. Advanced close coupled SCR compact mixer architecture. SAE Technical Paper 2015-01-1020. 2015. https://doi.org/10.4271/2015-01-1020
[37] Millo F, Sapio F, Paradisi BP et al. Experimental and numerical analysis of an innovative mixer geometry for urea injection in SCR applications. Emiss Control Sci Technol. 2022;8(1-2):78-95. https://doi.org/10.1007/s40825-022-00207-8
[38] Musa SNA, Saito M, Furuhata T et al. Evaporation characteristics of a single aqueous urea solution droplet. ICLASS. 2006.
[39] Pang Z, Chen R, Cao Y. Performance analysis and optimization for static mixer of SCR denitration system under different arrangements. Energies. 2022;15(23). https://doi.org/10.3390/en15238977
[40] Park T, Sung Y, Kim T et al. Effect of static mixer geometry on flow mixing and pressure drop in marine SCR applications. Int J Nav Arch Ocean. 2014;6(1):27-38. https://doi.org/10.2478/IJNAOE-2013-0161
[41] Payri R, Bracho G, Martí-Aldaraví P et al. Computational study of urea–water solution sprays for the analysis of the injection process in SCR-like conditions. Ind Eng Chem Res. 2020;59(41):18659-18673. https://doi.org/10.1021/acs.iecr.0c02494
[42] Payri R, Marti-Aldaravi P, Bracho G et al. Numerical analysis of the injection angle of urea-water sprays for the ammonia generation in realistic test conditions. SAE Technical Paper 2022-01-0584. 2022. https://doi.org/10.4271/2022-01-0584
[43] Popovac M, Hanjalic K. Compound wall treatment for RANS computation of complex turbulent flows and heat transfer. Flow Turbul Combust. 2007;78(2):177. https://doi.org/10.1007/s10494-006-9067-x
[44] Rogóż R, Kapusta ŁJ, Bachanek J et al. Improved urea-water solution spray model for simulations of selective catalytic reduction systems. Renew Sust Energ Rev. 2020;120:109616. https://doi.org/10.1016/j.rser.2019.109616
[45] Schaber PM, Colson J, Higgins S et al. Thermal decomposition (pyrolysis) of urea in an open reaction vessel. Thermochim Acta. 2004;424(1-2):131-142. https://doi.org/10.1016/j.tca.2004.05.018
[46] Schiller L, Naumann Z. A drag coefficient correlation. In: Z Ver Deutsch Ing. 1935;77(13-14):318-320.
[47] Tan L, Feng P, Yang S et al. CFD studies on effects of SCR mixers on the performance of urea conversion and mixing of the reducing agent. Chem Eng Process – Process Intensif. 2018;123:82-88. https://doi.org/10.1016/j.cep.2017.11.003
[48] Wang TJ, Baek SW, Lee SY et al. Experimental investigation on evaporation of urea-water-solution droplet for SCR applications. AIChE Journal. 2009;55(12):3267-3276. https://doi.org/10.1002/aic.11939
[49] Xu Z, Liu J, Fu J. Experimental investigation on the urea injection and mixing module for improving the performance of urea-SCR in diesel engines. Can J Chem Eng. 2018; 96(6):1417-1429. https://doi.org/10.1002/cjce.23082
[50] Ye J, Lv J, Tan D et al. Numerical analysis on enhancing spray performance of SCR mixer device and heat transfer performance based on field synergy principle. Processes. 2021;9(5). https://doi.org/10.3390/pr9050786
[51] Zhang C, Sun C, Wu M et al. Optimisation design of SCR mixer for improving deposit performance at low temperatures. Fuel. 2019;237:465-474. https://doi.org/10.1016/j.fuel.2018.10.025
[52] Zhao C, Lou D, Zhang Y et al. Application study on a new hybrid canning structure of after-treatment system for diesel engine. Energies. 2020;13(3). https://doi.org/10.3390/en13030734
[53] Zheng G, Palmer G, Salanta G et al. Mixer development for urea SCR applications. SAE Technical Paper 2009-01-2879. 2009. https://doi.org/10.4271/2009-01-2879
[54] Zhu N, Lv L, Ye C. Component analysis of deposits in selective catalytic reduction system for automotive diesel engine. MATEC Web Conf. 2016;51:03006. https://doi.org/10.1051/matecconf/20165103006

Bartosz Kaźmierski, MEng. – Faculty of Power and Aeronautical Engineering, Warsaw University of Technology, Poland.
e-mail: *bartosz.kazmierski.dokt@pw.edu.pl*

Łukasz Jan Kapusta, DEng. – Faculty of Power and Aeronautical Engineering, Warsaw University of Technology, Poland.
e-mail: *lukasz.kapusta@pw.edu.pl*